# PRECISION RADIAL VELOCITY SPECTROMETER

| | |
|---|---|
| **Document Title** | FORE-OPTICS FIBER ASSEMBLY |
| **Document Number** | PRVS-TRE-00002-0001 |
| **Issue** | 1.0 |
| **Date** | 16th September 2006 |

| | | | |
|---|---|---|---|
| **Document Prepared By:** | L. Ramsey & L. Engel | **Signature and Date** | L. Ramsey & L. Engel<br>September 14, 2006 |
| **Document Approved By:** | David Lunney | **Signature and Date** | David Lunney<br>September 16, 2006 |
| **Document Released By:** | David Lunney | **Signature and Date** | David Lunney<br>September 16, 2006 |

| | |
|---|---|
| Document Number: | PRVS-TRE-00002-0001 |
| Issue: | 1.0 |
| Category: | Technical Report |
| Status: | Issued |
| Author: | L Ramsey, L Engel |
| Date: | 16th September 2006 |

## CHANGE RECORD

| **Issue** | **Date** | **Section affected** | **Change Description** |
|---|---|---|---|
| 0.2 | 10 Sept 06 | All | Clarifications, add modal noise estimates & figure 3 change |
| 0.3 | 12th September 06 | All | Revision by DWL |
| 0.4 | 14th September 06 | All | Grammar and references by L Ramsay |
| 1.0 | 14th September 06 | | Final review before issued to Gemini by DWL |
| | | | |
| | | | |
| | | | |
| | | | |
| | | | |
| | | | |

# Table of Contents



# List of Figures

# List of Abbreviations

| | |
|---|---|
| A+G | Gemini acquisition and guidance system |
| FDAS | Fiber Deployment and Acquisition System |
| FPRD | Functional and Performance Requirements Document |
| FOV | Field of view |
| FRD | Focal Ratio Degradation |
| GCAL | Gemini facility calibration unit |
| HET | Hobby-Eberly Telescope |
| HR | High (spectral) resolution |
| NA | Numerical Aperture |
| OAP | Off-axis parabola |
| OCDD | Operation Concepts Definition Document |
| PRVS | Precision Radial Velocity Spectrometer |
| PSF | Point spread function |
| R | Spectrograph resolving power |
| RV | Radial velocity |
| S/N | Signal-to-Noise ratio |
| XD | Cross-dispersed |

# Definitions

| | |
|---|---|
| TBD | To Be Defined : a requirement to be developed during the preliminary design stage of the instrument. |
| TBC | To Be Confirmed : a requirement that is correct with the current design information but requires confirmation during the preliminary design stage of the instrument. |
| TBR | To Be Reviewed : a requirement specified to meet the PRVS top-level requirements, but which might over-constrain the design. |

# PRECISION RADIAL VELOCITY SPECTROMETER

| | |
|---|---|
| Document Number: | PRVS-TRE-00002-0001 |
| Issue: | 1.0 |
| Category: | Technical Report |
| Status: | Issued |
| Author: | L Ramsey, L Engel |
| Date: | 16th September 2006 |

## 1. PURPOSE

This document describes the concept design and fabrication issues for Fore-Optics Fibre Assembly as well as its interfaces with other subsystems of the PRVS. We also outline key properties of optical fibres that are relevant to this system.

## 2. APPLICABLE AND REFERENCE DOCUMENTS

| Reference | Document Title | Document Number | Issue / Date |
|---|---|---|---|
| AD01 | Science Case | PRVS-SPEC-00004-0001 | 1.0 |
| AD02 | Science Requirements | PRVS-SPEC-00005-0001 | 1.0 |
| AD03 | Fibre Deployment and Acquisition System | PRVS-TRE-00007-0001 | 1.0 |
| AD04 | Calibration Assembly | PRVS-TRE-00004-0001 | 1.0 |
| AD05 | Spectrograph Sub-System | PRVS-TRE-00003-0001 | 1.0 |

# 3. FORE-OPTICS FIBER ASSEMBLY

The Fore-Optics Fiber assembly is effectively the fore-optics to the PRVS spectrograph and consists of the fiber cable from the Fiber Deployment and Acquisition System (FDAS) down to and into the Spectrograph Assembly to the Fiber slicer. It also includes the fiber cable from the Calibration Unit to both the spectrograph slit and the calibration input in the FDAS Unit. The blue shaded area in Figure 1 below demarcates the Fore-Optics Fiber Assembly within the entire PRVS systems concept.

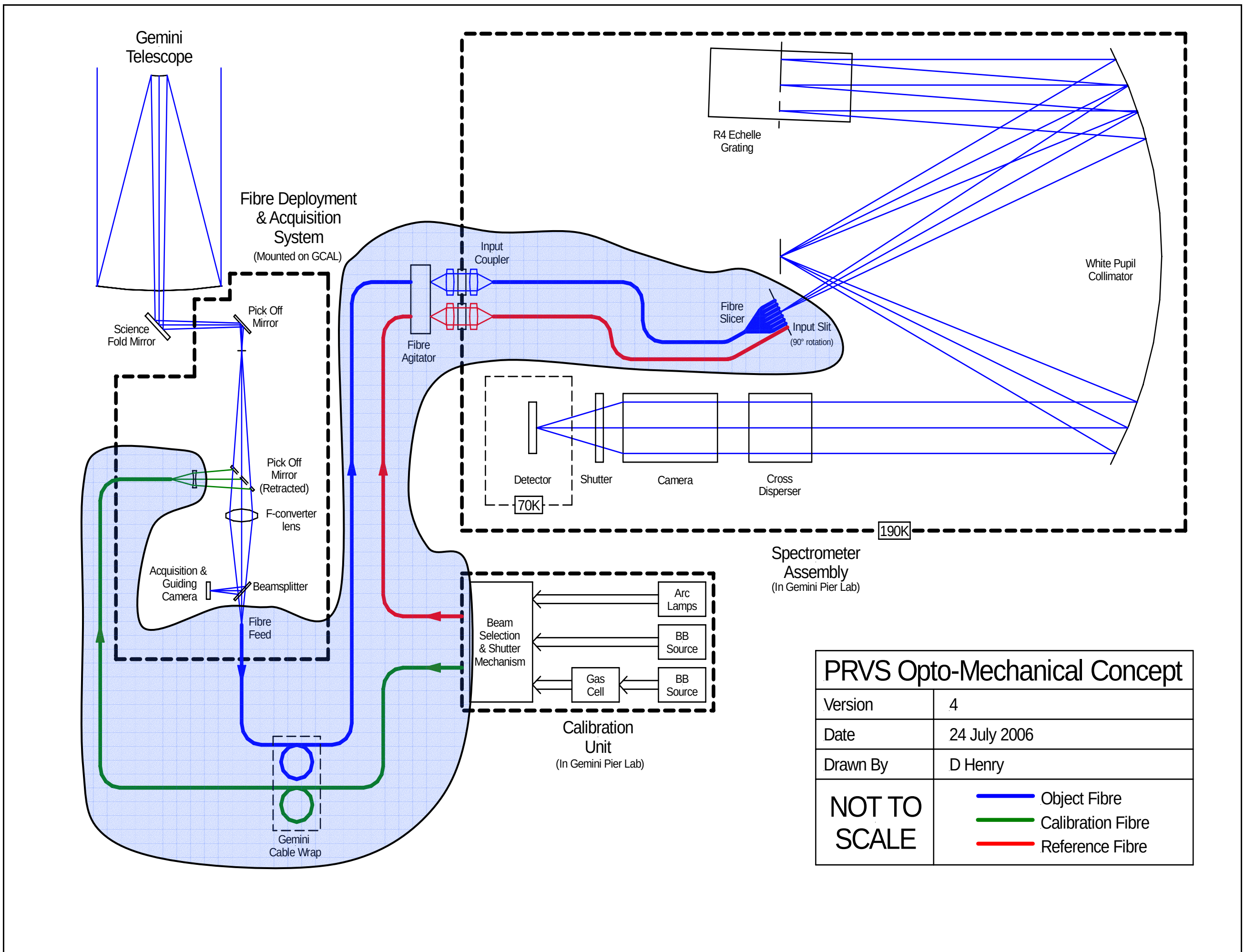


**Figure 1: Instrument Layout**

## 3.1 KEY PROPERTIES OF OPTICAL FIBERS

Fundamental to the performance of the PRVS is the fact that the optical signal is transported to the spectrograph via an optical fiber. While fibres have some drawbacks as we will detail below they also have one substantial advantage for precision radial velocity measurements; modal scrambling. Below we will discuss key properties of the fused silica core, doped fused silica clad multimode fibres which are the type we will employ exclusively in the PRVS. A good review of fiber properties is Schotz et al ( in Fiber *Optics in Astronomy III*, ASP Conference Series, Vol. 152, p20-31, 1998). We are using as a baseline Polymicro Technologies fibres as our experience has shown this manufacturer's products deliver superior Focal Ratio Degradation (FRD). Figure 2 shows the standard product list for the Infrared optimized fibres of the type which we will use. The fiber number is core/cladding/buffer diameter. Thus a FIP300330370 fiber has a 300 micron core with 15 micron thick cladding giving a diameter of 330 microns and a 20 micron thick Polyimide buffer giving a final diameter of 370 microns. The FDAS produces a 1.4 arc-second field into a 300 micron diameter spot which enables us to utilize a standard 300 mm core fiber. While it may be possible to use a standard product we do need to carefully asses the validity of the rule of thumb that states that the cladding should be ~10x the wavelength for the lowest attenuation as noted in the above cited reference by Schotz et al. From Figure 2 one can see that the there are two standard cladding/ core ratios of 1.1 and 1.2. This ratio is set in the preform from which the fiber is drawn. Thus we could use a special draw of a 1.2 ratio perform to get a 300360400 fiber.

| Product Descriptor | Core (μm) | Clad (μm) | Buffer (μm) |
|---|---|---|---|
| FIP100110125* | 100 ± 3 | 110 ± 3 | 124 ± 3 |
| FIP150165195 | 150 ± 3 | 165 ± 3 | 195 ± 5 |
| FIP200220240 | 200 ± 4 | 220 ± 4 | 239 ± 5 |
| FIP300330370 | 300 ± 6 | 330 ± 7 | 370 ± 10 |
| FIP400440480 | 400 ± 8 | 440 ± 9 | 480 ± 7 |
| FIP500550590 | 500 ± 10 | 550 ± 10 | 590 ± 10 |
| FIP600660710 | 600 ± 10 | 660 ± 10 | 710 ± 10 |
| FIA8008801100** | 800 ± 20 | 880 ± 15 | 1100 ± 30 |
| FIP100120140 | 100 ± 3 | 120 ± 3 | 140 ± 4 |
| FIP200240280 | 200 ± 4 | 240 ± 4 | 275 ± 5 |
| FIP320385415 | 320 ± 8 | 385 ± 8 | 415 ± 10 |
| FIP050070085 | 50 ± 2 | 70 ± 2 | 85 ± 3 |
| FIP100140170 | 100 ± 3 | 140 ± 3 | 170 ± 5 |
| FIA100011001300** | 1000 ± 20 | 1100 ± 15 | 1300 ± 40 |

* Not recommended for wavelengths greater than 1000nm.
** Acrylate buffer

**Figure 2: Stocked Fiber List from Polymicro Technologies**

### 3.1.1 Transmission

Modern optical fibres are very close to their theoretical Rayleigh scattering limit for transmission in visible and red out to about 1.7 microns. At the short wavelength end, metal impurities increase the attenuation above the Rayleigh limit and in the red, OH absorption complexes limit transmission. As light attenuation is key in all commercial application of fibres, manufacture's produce high quality data for this parameter. Figure 3 shows the attenuation for an IR optimized Polymicro FI type fiber. Over the 0.99 to 1.75μm band pass of the PRVS, the attenuation is less than 3 db/km with the exception of the absorption peak at 1.38 μm. In Figure 4 we show the transmission for various lengths of fiber cable. With cable lengths up to 75 meters, the loss over the PRVS bandpass is less than 5% except for the region between 1.36 and 1.418 μm which is also in a region of strong telluric absorption. This figure includes only the loss due to material absorption and scattering and does not include waveguide leakage. Waveguide leakage should be small in a properly designed cable where the bend radius is controlled.

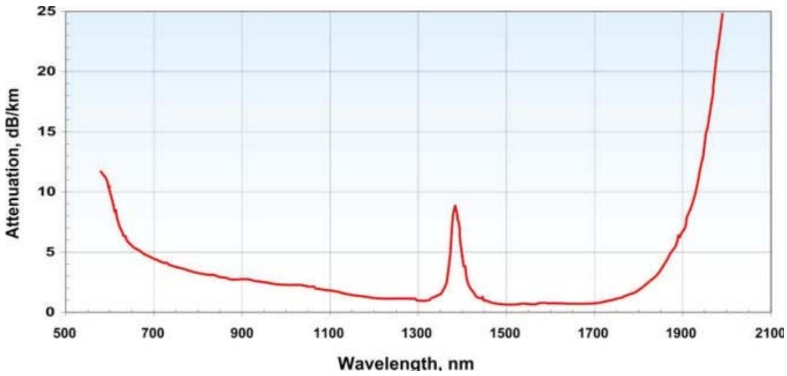


**Figure 3: FI type fiber attenuation in NIR**

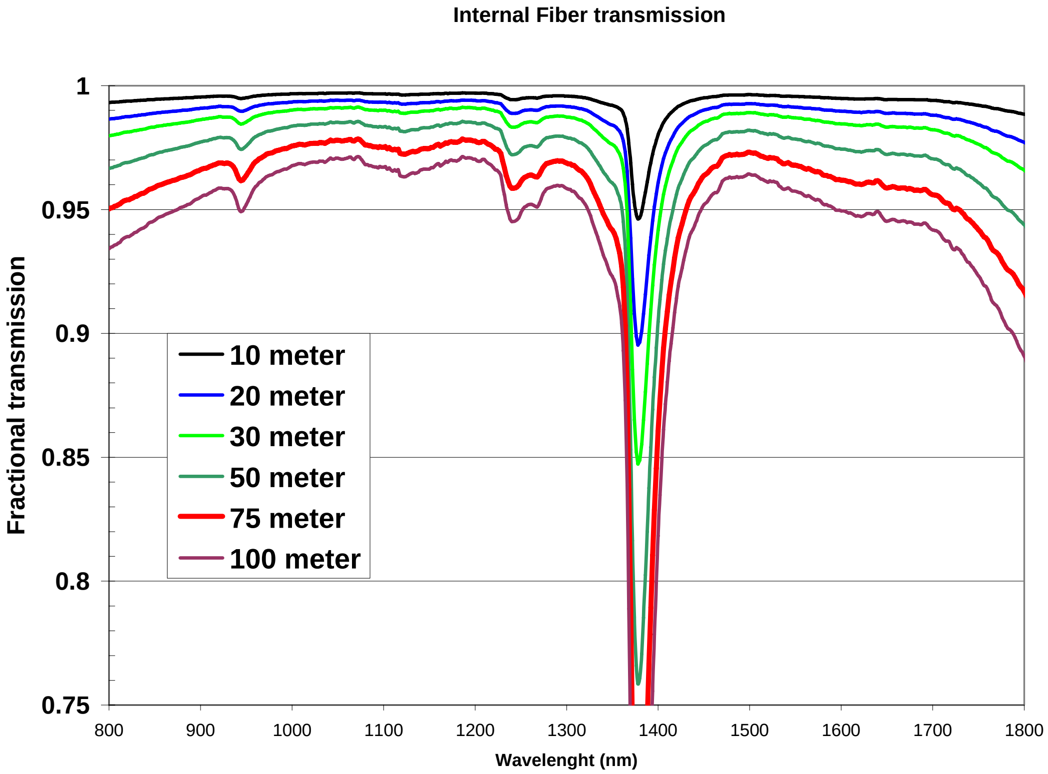


**Figure 4: Transmission of various lengths of Fiber in NIR**

The transmission for the various lengths displayed in Figure 4 assume no unusual loss mechanisms and especially assume a cladding thickness of at least 18 microns; i.e. 10 times the longest wavelength transmitted. The Polymicro standard 300 micron core fiber has a 330 micron cladding diameter and thus only a 15 micron thick cladding. The 10 times is just a rule of thumb and once the nominal length of the cable is known, we will conduct tests to assure good transmission out to 1.75 microns for the modal distribution we envision.

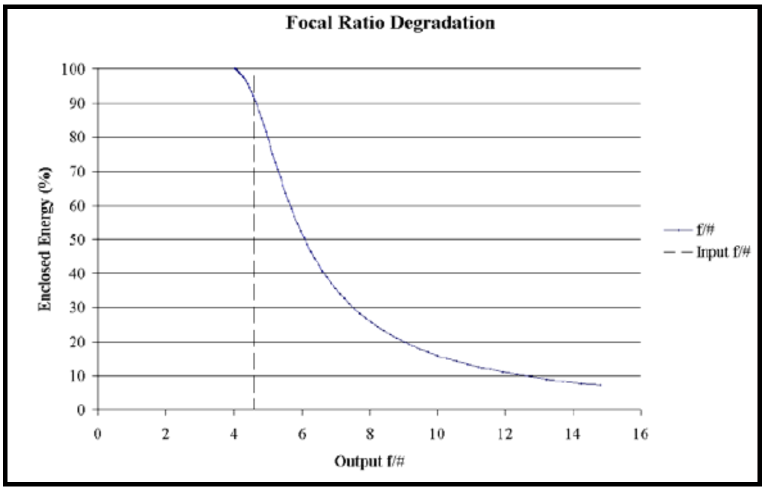


**Figure 5: FRD in a fiber with a f4.6 input as used at HET**

### 3.1.2 Focal Ratio Degradation

Focal Ratio Degradation (FRD) is a property of optical fibres that is typically more important to astronomers than other users and is effectively due to the redistribution of modes in a fiber due to a number of factors including irregularities in the core-cladding interface, variations in the diameter of the core and cladding as well as bending of the fiber (Nelson, *Fiber Optics in Astronomy I*, ASP conference Series, Vol. **3**, p2-22, 1988). While in reality fibres are optical waveguides and a rigorous description of modes must employ electromagnetic theory, a reasonable way to envision a mode is geometrical as a ray of light hitting the input face of a fiber at a particular angle. A beam of a given f/ratio has a distribution of modes over solid angles and position dictated by that beam and the image size on the fiber. As the light propagates there is modal dispersion that can be characterized by an increase spread in the angles at the output of the fiber which is a smaller f/ratio; thus FRD. A nice description and references to prior literature is given by Carrasco and Perry (*MNRAS* volume **271** 1-12, 1994). FRD properties of fibres essentially dictate that the insertions f/ratios be relatively fast; certainly less than f/8. Experience has shown that FRD can be held to 10% or better using insertion f/ratios between 4 and 6 and care in the construction of fiber cables, especially terminations. Figure 5 shows measurements for a 300 micron fiber that is currently in use on the Medium Resolution Spectrograph (MRS) at Hobby-Eberly telescope (HET) which has a 13% loss due to FRD. We adopt a similar goal for the PRVS. For an insertion f/ratio of 5.5 we have a design goal of 97% of the light within f/5.

### 3.1.3 Scrambling

Fiber scrambling is related to FRD as the basic mechanism of scrambling is modal dispersion. Figure 6 is an illustration of far-field scrambling in a fiber with excellent FRD from actual measurements with the HET pupil simulator at Penn State. As the top row of images show a simulation of the HET pupil at various positions during a track ( for a description of HET see Ramsey et al. Proceedings of SPIE Conf. 3352, *Advanced Technology Optical Telescopes V*, Kona HI, March, 1998.p. 34-43 ). The bottom row

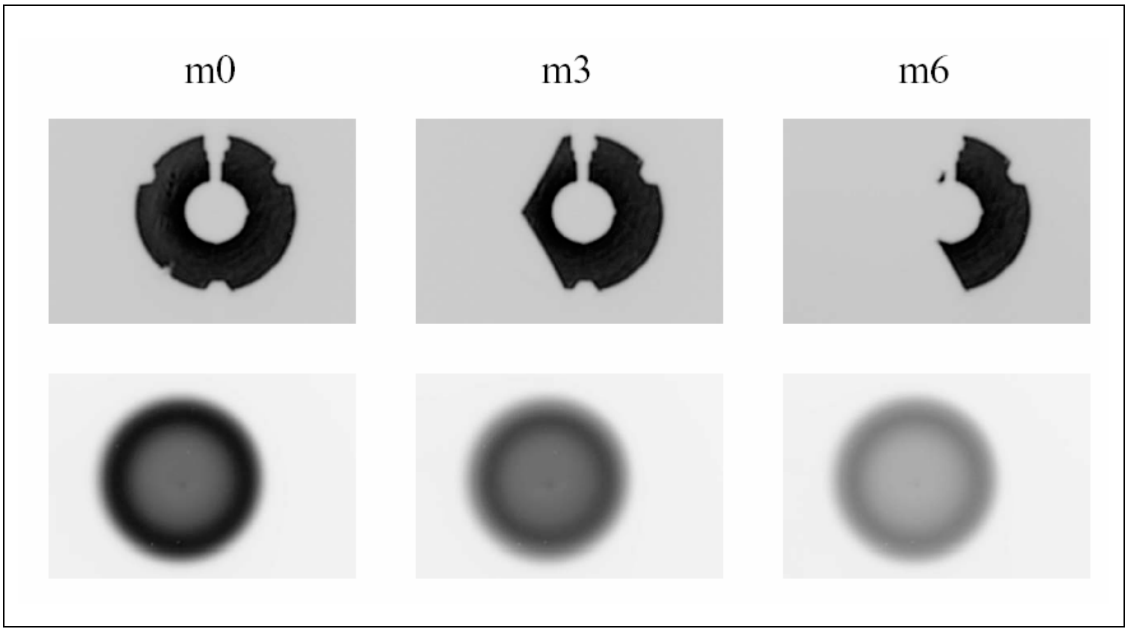


**Figure 6: Illustration of scrambling**

of images show the far field pattern of the fiber fed with an f/4.6 beam defined by image **m0, m3 and m6** respectively. It appears the scrambling is good with the dominant visual differences in intensity is as expected. However, closer analysis does reveal subtle differences in the modal distribution and these could lead to variations in the PSF which would be reflected in the radial velocity accuracy due to changes in the effective photocenter of the image of the fiber on the detector. As we are looking at variation on the order of $10^{-3}$ pixel, extremely good scrambling is essential. Hunter and Ramsey (PASP **104**, 1244-1251, 1992) discuss measurements of an optical double scrambler to increase scrambling by up to an order of magnitude. In a very interesting recent paper Avila et al. (SPIE, Orlando, 2006) show that excellent scrambling may be achieved with mechanical agitation. Mechanical agitation required to control modal noise (see section 3.1.4) is an extremely attractive alternative to optical scrambling as the latter extracts a throughput penalty.

### 3.1.4 Modal Noise

Modal noise can arise when modal dispersion varies during and between exposures when there are a relatively small number of modes. In the case where a fiber is absolutely static, modal noise should not be a consideration. A good laboratory illustration of modal noise is to look at the *change* in a speckle pattern in a fiber illuminated by a laser that undergoes the least bit of disturbance. This can lead to the measured S/N in a fiber spectrograph being significantly less than that expected from pure photon statistics. Baudrand and Walker (PASP 113, 851, 2001) and Grupp (A&A 412 897, 2003) discuss modal noise in visible spectrographs and use experimental results to model the effects on the achievable S/N in the presence of modal noise. The number of modes in a fiber is proportional to the area of the fiber core and the $NA^2$ and inversely proportional to wavelength or:

$$N_\lambda = 0.5(\pi\ D\ NA\ \lambda^{-1})^2 .$$

Figure 7 compares the number of modes for the two sizes of fibres being considered for the PRVS. For each fiber size we show the modal number possible with the 0.22 NA of the fiber as well as the number for the NA=0.1 (f/5) which the fibres will output to the spectrograph. The calibration fibres will have mechanical pressure-type mode scramblers to allow all modes available in a 0.22 NA fiber to be filled. This will help guarantee a stable illumination pattern from the calibration fibres.

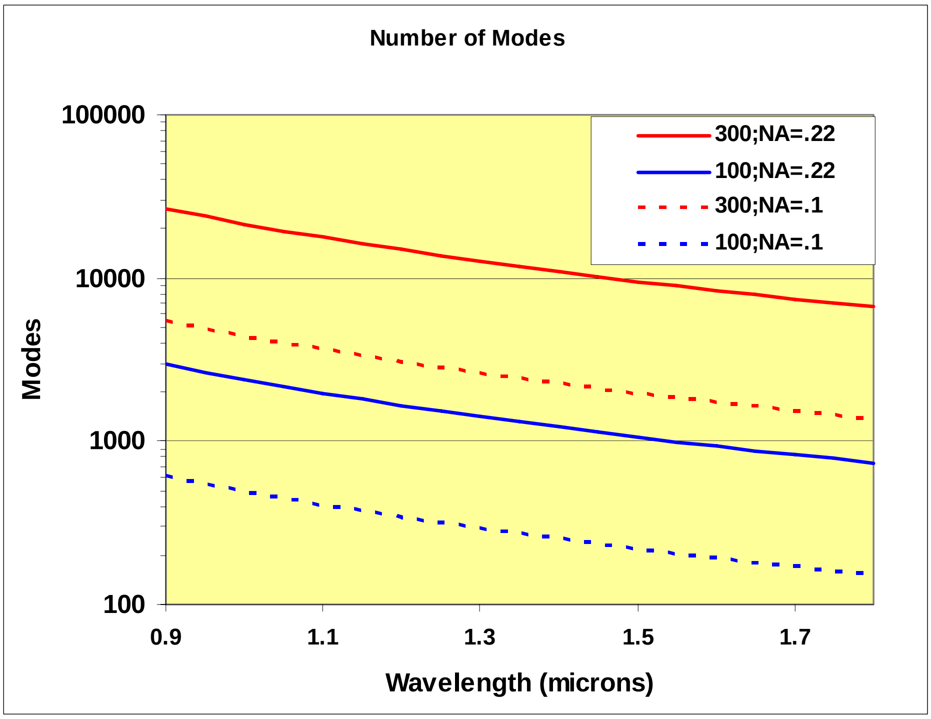


**Figure 7: Predicted number of modes for 100 and 300 micron core fibres for 0.1 and 0.22 NA.**

For the 100 micron fiber in the slicer, the number of modes is small per fiber. However there are seven fibres and we should have at least 1000 modes at the longest wavelengths. The single calibration fiber will be the most modally impaired. We estimate the achievable S/N using the Baudrand and Walker model, which is the most pessimistic. They model the modal noise limited S/N, $(S/N)_{limit} = (N_\lambda)^{0.784}$. In **Error! Reference source not found.** we look at the modal noise limited S/N for both a 300 and 100 micron core fiber as well as seven 100 micron core fibres using this approximation. Their data extended from 0.5 to 0.95 microns thus we are extrapolating a factor of 2 out to our long wavelength limit. The model results in **Error! Reference source not found.** clearly indicate a problem especially for the single 100 micon calibration fiber. Fortunately, both Baudrand and Walker and Grupp demonstrate that mechanical agitation of the fiber removes much of the deleterious effects of modal noise.

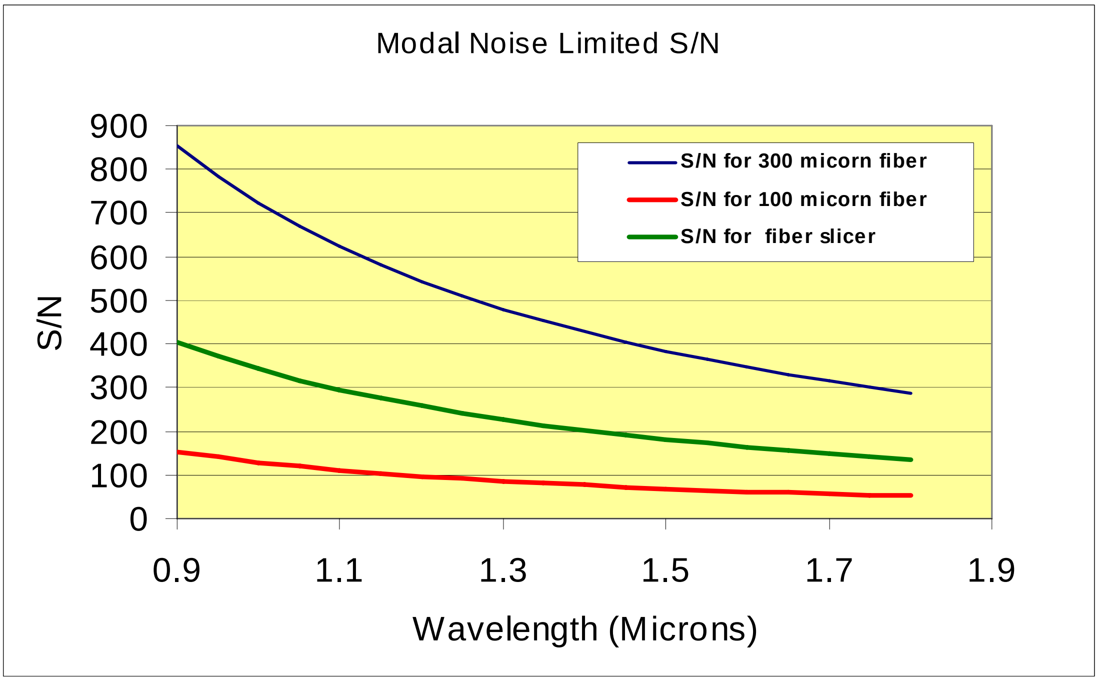


**Figure 8: Modal noise limited S/N**

**We have conducted some very preliminary tests to verify that the mechanical agitation remedy works in the NIR.**

Figure 9 shows a series of three frames. All these frames are ratios of consecutive flat field exposures on the PRVS pathfinder experiment at Penn State in the Y band about 1.07 micron. Frame 1 is a ratio of consecutive flat fields with no disturbance between exposures. As expected the ratios leave virtually no signature. Ignore the noisy upper right quadrant which had some noise pick-up since eliminated. Frame 2 is a similar ratio where the fiber was disturbed between the exposures. The ratio clearly demonstrates increased noise due to the change in the modal distribution between exposures. The fluctuations are large, about 7%. This exaggerated signature of modal noise is due in part to the high degree of vignetting on the grating and elsewhere in this brass-board instrument. Grupp discusses these effects in his study. Frame 3 shows the effect of using a 60 Hz vibrator on the fiber between exposures and no signature of the modal noise remains. These results support our use of mechanical agitation for modal noise control in our baselin

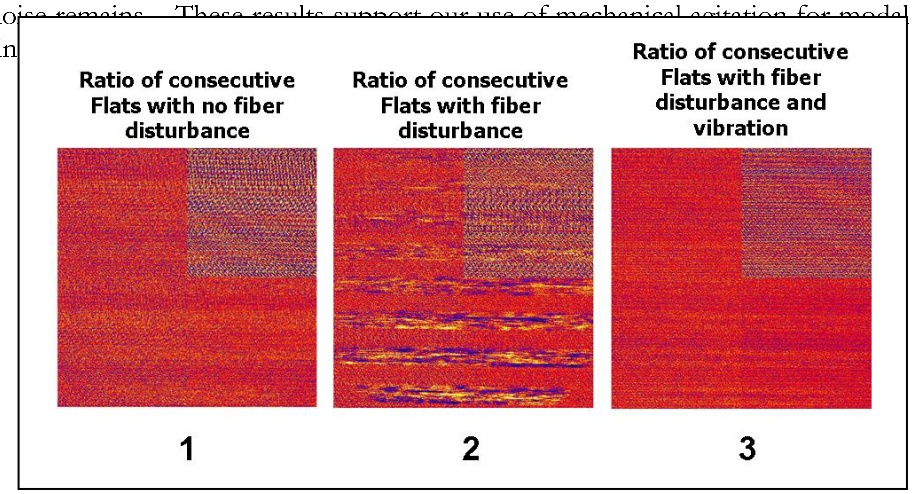

**Figure 9: Modal Noise tests in Y band.**

## 3.2 DESIGN APPROACH FOR THE FORE-OPTICS FIBER ASSEMBLY

### 3.2.1 System Summary

The baseline concept for the Fore-Optics Fiber System is illustrated in Figure 10. The fibre input is the f/5.5 beam from FDAS is imaged onto the input of the science fiber. This fiber and accompanying cable held by the Ferrule Attachment assembly which is fixed firmly to the FDAS module. The light first goes through a glass plate attached to the end of a ferrule via an index matching gel and then directly into a

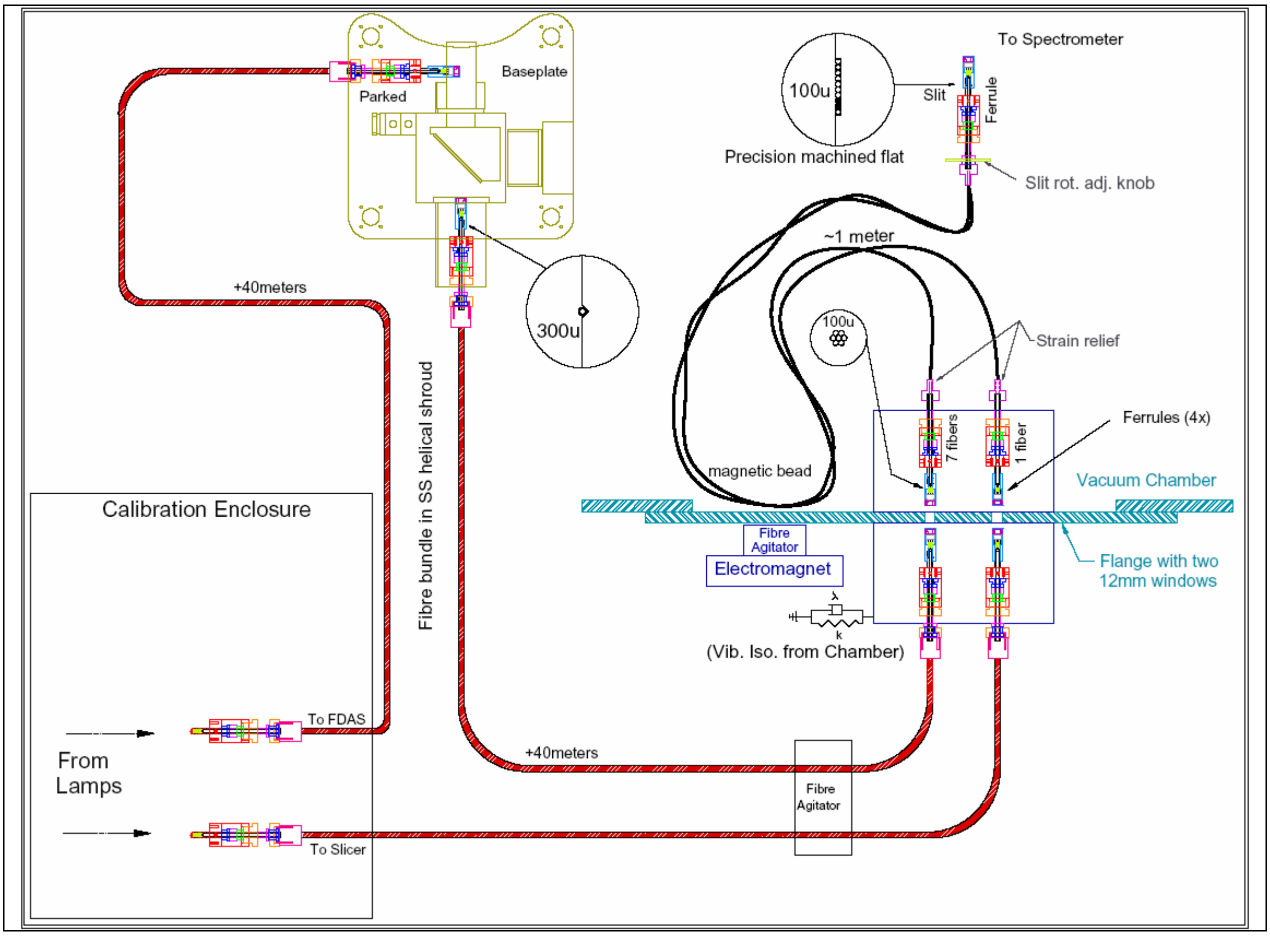


**Figure 10: Conceptual Schematic of the Fore-Optics Assembly**

FIP 300330370 µm core/clad/buffer 0.22 NA fibre cable. A Stainless Steel ferrule, see section 3.2.4, holds the fibre in place by epoxying the fibre only near the end of the ferrule. This scheme is identical at both the input and the output end and is integral to our effort to minimize (FRD). The +40meter fibre cable is then routed to the basement of the telescope to an enclosed Invar breadboard which is subsequently attached to a flange on the vacuum chamber. The fibre is slightly vibrated near the end to randomize fibre modal structure. The fibre mounts are bilaterally attached to the flange such that they minimize rotational and translational deltas due to temperature or pressure changes. Here the output of the fibre ferrule, with associated lenslet, is held for alignment, see section 3.2.3. Again the only point of attachment of the fibre is at the very end of the ferrule. The collimated beam then goes through the 12mm diameter vacuum chamber window to a lenslet on the end of the ferrule. This approximate f/5.5

lens images the output of the single 300 mm fiber onto an array of seven circularly packed 100/110um core/clad 0.22NA fibres which make up a fiber slicer; see section 3.2.7.2. There is about 1 meter of fiber from the slicer input to the fiber pseudo slit. This cable is run through magnetic beads that can be slightly vibrated through the chamber wall via an electromagnet outside the chamber. Finally the output end of the pseudo slit is butted to a parallel fused silica plate through an index matching vacuum compatible gel. This is the output of the Fore-Optics Fiber assembly which is in turn re-imaged on the to spectrograph entrance slit.

A calibration fibre cable is needed to continuously have a reference spectral point. There are two paths for the calibration output as described in PRVS-TRE-00004-0001. One is directly to enclosed Invar breadboard which is subsequently attached to a flange on the vacuum chamber. Similar to the science fiber it is collimated by a lens on the end of the ferrule enters the spectrograph through a 12 mm window. Where the science fiber is imaged on the fiber slicer, this calibration fiber output is imaged onto a 100 micron core fiber which is bundled with the slicer fibres though the magnetic bead agitator to the pseudo slit.

The second calibration cable path uses a cable fabricated identically to that for the science fiber to carry calibration signals up to the Fiber Deployment and Acquisition System. Instead of a flat protective plate the FDAS end, the calibration fiber has a lens which generates an expanding beam which is folded 90 degrees so that in the stowed position the FDAS pick-off mirror directs it to the f/5.5 re-imaging lens onto the science fiber.

### 3.2.2 Interface with Fiber Deployment and Acquisition system

The FDAS is described in a separate document (PRVS-TRE-00007-0001). Here we briefly describe the interface with that system. Figure 11 reproduces a drawing from PRVS-TRE-00007-0001. In it we note on the two interfaces. The circle labelled **1** shows where the science fiber attaches to this assembly. This is designed for self-aligning attachment and easy removal. The stainless Steel block, which holds the ferrule, is fitted to FDAS and remains attached. The ferrule lateral movement is constrained by the fit between the ferrule and clearance hole in the block. The tight tolerance between the tow parts ensures a relatively close fit every time. Set screws further ensure this quick yet close self aligning occurs. The circle labelled **2** shows the position where the fiber from the calibration unit attaches. When in the parked position the calibration ferrule feeds into the PRVS fibre feed to the pick-off mirror via a 12.7mm fold mirror.

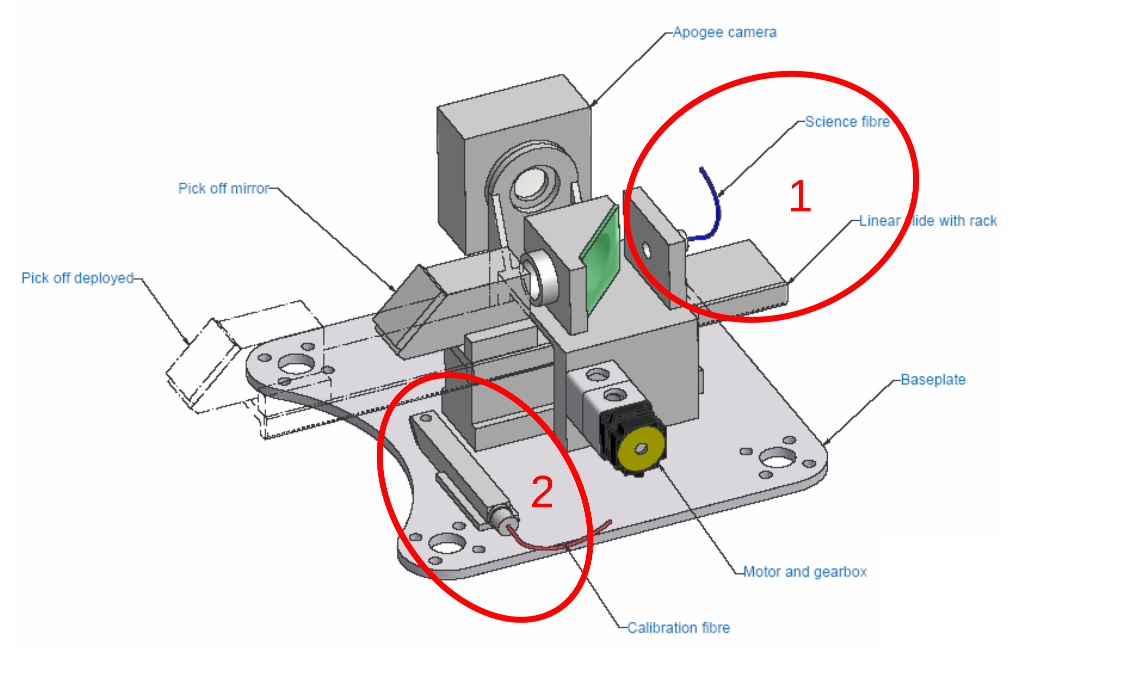


**Figure 11: Interface with Fiber Deployment and Acquisition system**

### 3.2.3 Fiber Attachment Assembly

The stainless steel spiral wrap is attached to the ferrule via a large threaded nut. The spiral wrap has a male threaded end that is threaded to the large nut shown on the left side of the Figure 12. This threaded nut has a clearance hole to the ferrule sleeve which is allows rotation around the ferrule and also some slight axial movement. Holding this in place is a nut, sleeve and lock nut. Attaching the ferrule to the stainless steel block is another large nut with a center clearance hole; it is denoted as the tightening nut in Figure 12 & Figure 13. Abutting against this nut is an assembly of four parts (sleeve, knurled lock nut, nut, & sleeve) which are adjusted left or right only once for focusing and then locked in place. Hence to remove fibre cable after adjustment it only requires removal of the tightening nut and the subsequent reinsertion just requires tightening with the ferrule remaining in the same axial position as before. The ferrule has a tight fit to the stainless steel block such that the transverse alignment is maintained also. The use of one of the three set screws are there only for ease of the initial focus adjustment and can remain there afterwards as explained in 3.2.2. At the end of the ferrule is a cylinder containing either a lenslet or glass plate depending upon where it is located in the assembly. Please note that between the lenslet or glass and the fibre is an index matching gel, also that all ferrules and cylinders are essentially the same for ease of manufacturing and assembly. The lenslet cylinder is threaded onto the ferrule. We will specify the tolerances on both the ferrule and the lenslet cylinder tightly to assure alignment of the fiber output face on the axis of the collimating lens. The lenslet holder is threaded on the ferrule first, with the gel and lenslet going on next. These are held in place by the lenslet nut being threaded into the cylinder as shown on upper view on the right side of the figure. Finally, the stainless steel block is held in place by the threaded holes at the base of the block. It can either be side or bottom mounted depending upon the location of the interface holes.

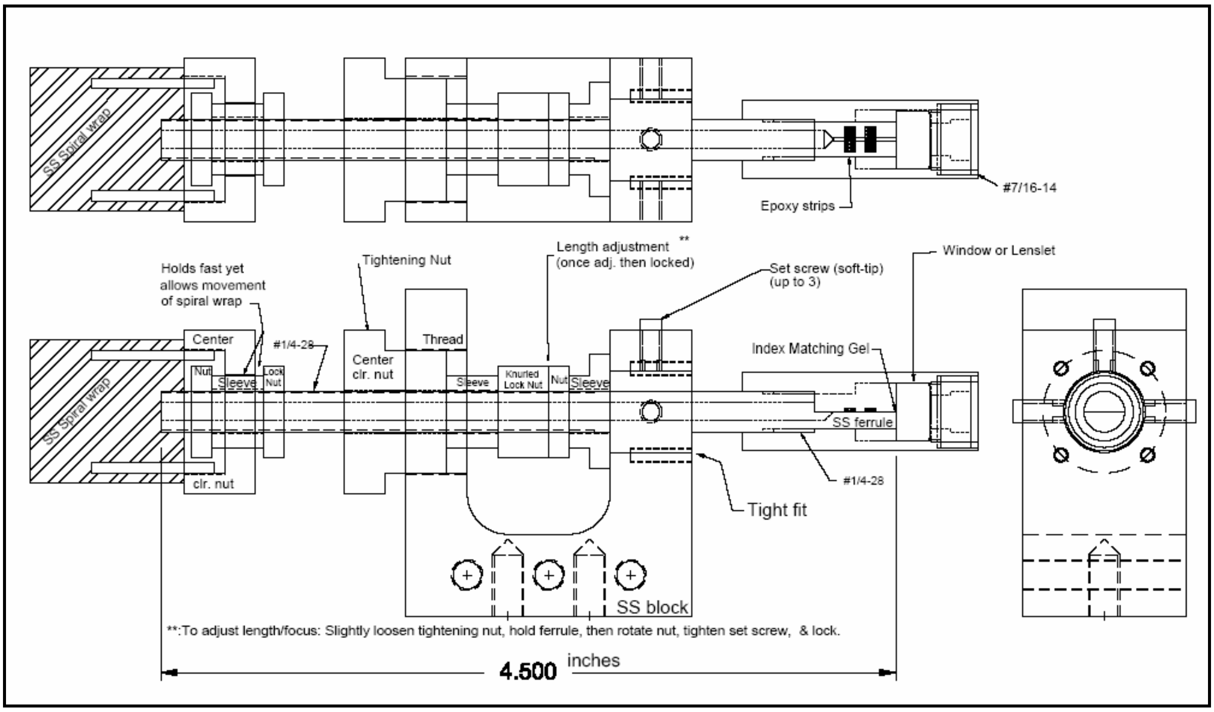


**Figure 12: Fiber attachment Assembly Detail**

The fibre ends are held in place by thin epoxy strips to reduce FRD. In addition the fibre cable outer PVC sleeve, Kevlar mesh and inner Hytrel sleeve (TBD-not shown) has room to move within the spiral wrap and is strain relieved at the end of the ferrule, again to reduce FRD.

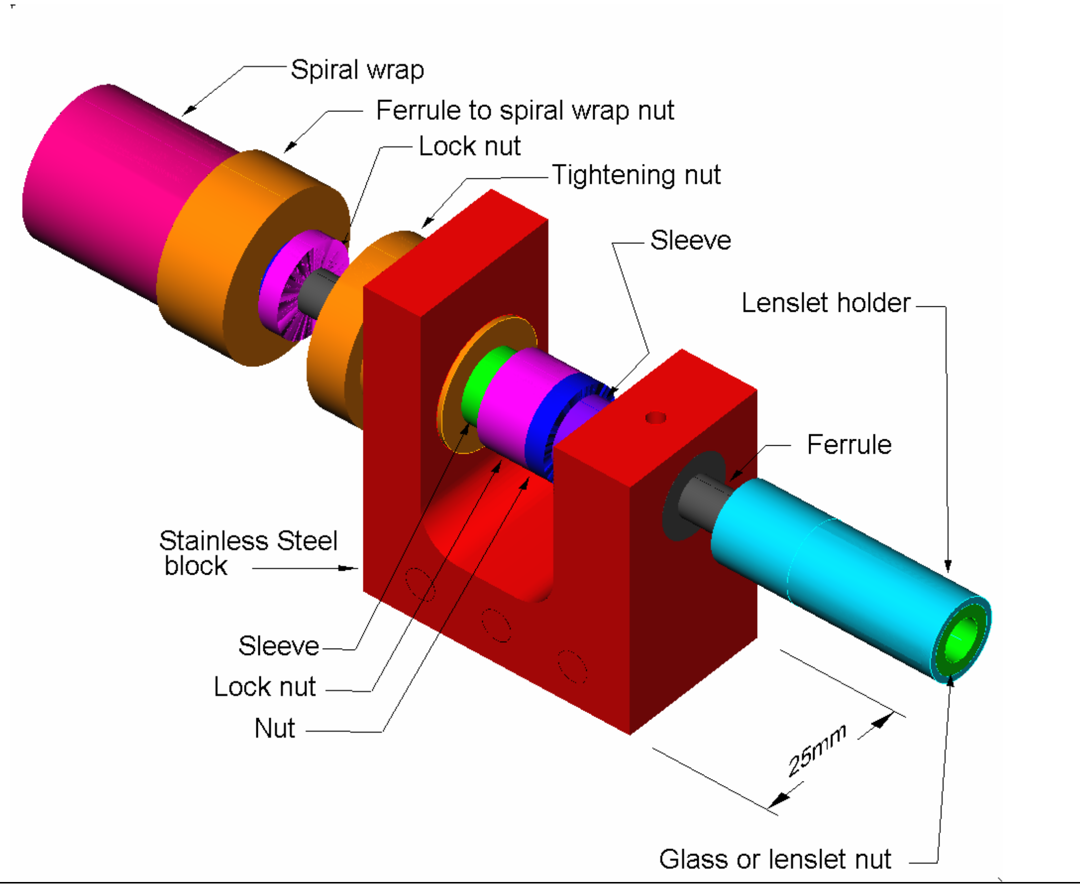


**Figure 13: Fiber Attachment Assembly Detail II**

### 3.2.4 Fiber Ferrules

For single fibres we have used a basic fiber ferrule scheme. This is illustrated in Figure 14 for a laboratory brass ferrule; we would used stainless steel for all PRVS ferrules. In this scheme a circular rod has a hole drilled through until the last 12-15 mm. This last bit at the input end of the ferrule is milled half off and a precision V groove to hold the fiber is cut along the axis. Key to controlling FRD is to minimize stress when attaching the fiber. We typically use two narrow (1-3 mm wide) strips of low shrinkage UV curing epoxy (Nordlund 68) to attached the fiber. We may polish in the same ferrule in which case a larger amount of this epoxy is mounded on the end surrounding the fiber. This is dissolved away with Acetone before final use.

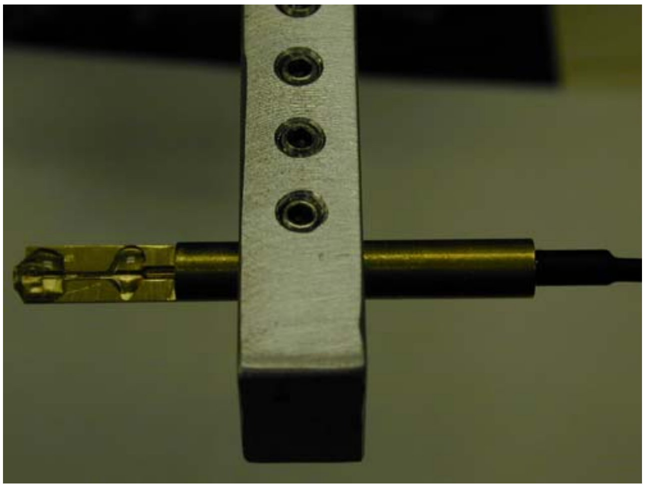

**Figure 14: Fiber-Ferrule attachment example**

### 3.2.5 Fiber Cable

The fiber cables from the FDAS to the spectrograph room will be similar in construction (and perhaps a single cable depending on routing). The Polyimide buffered fibre cable has a loose Hytrel® sleeve covered with PVC and a Kevlar® weave for strength. It also has an unattached Stainless Steel over-jacket (AKA- helical shroud) to maximize bending radii and minimize breakage which also reduces stresses and micro-cracking problems.

### 3.2.6 Spectrograph Fiber Feed Through

The vacuum chamber fibre cable feed through, see Figure 10, can be accomplished via small plate glass windows, one larger window, vacuum tight direct feed-throughs or some other technique. The present method has the ferrule and associated lenslet assembly attached to an aluminium flange in the bottom of the vacuum chamber. The ferrules on the inside of the chamber are attached to a small Invar breadboard which is attached to the flange. On the exact opposite side of the flange, outside of the chamber, are the science and calibration ferrule assemblies which also mounted on an Invar breadboard. This mounting technique reduces any rotational or translation misalignment for changes in vacuum chamber pressure or temperature.

### 3.2.7 Fiber Slicer and spectrograph pseudo slit

The 1.4 arc-second 300 micron fiber that brings the light from the Fiber Deployment and Acquisitions System to the spectrograph would result in a resolving power of only 24,000 with the spectrograph. The option is to increase the spectrograph beam size a factor of 3, and thus the volume by nearly an order of magnitude. Alternatively we can get a more narrow effective slit width by placing a slit over the fiber or use an image slicer to reduce the effective slit width about a factor of three. By placing a slit over the fiber, or re-imaging the fiber onto a slit the fraction of light entering the fiber that would make it through the appropriate slit width is about 33%. We argue that an image slicer will yield at least a factor of two more.

#### 3.2.7.1 Image Slicer vs. Fiber Slicer

There are two technical approaches to an image slicer in this application. One is a Bowen-Walraven slicer. And the second is to use a fiber bundle. Bowen-Walraven type slicers are used on FEROS, UVES and bHROS. Dekker et al. (SPIE 4842-28) discuss UVES image slicers and give an efficiency of 79% for a 3 slice image slicer similar to what we would have to employ and Avila et al. (SPIE, Orlando, 2006) notes a two slice image slicer is used on FEROS. The FEROS on-line documentation for the device has an estimate, not measured, efficiency of 90%. A Bowen Walraven type slicer makes use of multiple internal reflection of the a circular image where at each reflection part of the image is allowed to exit the prism leading to a pseudo slit image as shown on the right in Figure 15 for the case of a three slices. The red shaded region of each circle is the sliced image compared to a rectangular slit; also shaded red. It should be noted that as only one slice can be strictly in focus, these work best in slow beams. Thus the ~f/5 beam exiting the fiber would need to be re-imaged on to the slicer at a longer focal ratio. For the PRVS, this would be f/14 to match that of the collimator. The pseudo slit for a fiber slicer consisting of seven 100 μm core diameter and 110 micron cladding diameter is illustrated on the left in Figure 15.

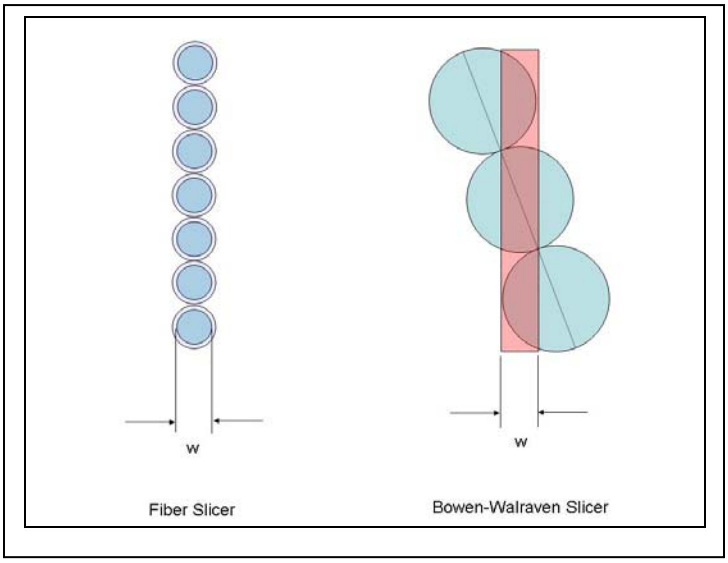


**Figure 15: Image Slicer Slit Formats**

Assuming we can make the fiber slicer with 100/110/stripped buffer fibres, the best expected transmission is limited by the packing fraction geometry; in this case ~68%. Given the numbers cited above for the UVES slicer, that is only 80% of what might be expected of a Bowen-Walraven. However, the advantage lies in a more uniform PSF across the slicer and, as we will see below a better way to insert a calibration emission line spectrum into the spectrograph.

#### 3.2.7.2 Fiber Slicer Concept and Fabrication

The baseline concept for the PRVS image slicer and integral calibration fiber is illustrated in Figure 16. We will use seven Polymicro FIA 100/110/250 fibres which have Acrylate buffers for the slicer. While the fiber core and cladding are standard sizes, the buffer is not and will require a special order. The buffers are stripped with Acetone for a few cm and the ends fit into a precision stainless steel tube that is holds the fibres in a tight hexagon shape. A separate 100 micron core fiber which is fed from the calibration system joins the bundle which is terminated at the pseudo slit. Here the seven fibres from the slicer and the single calibration fiber are placed in a ferrule that allows them to form a flat line. The calibration fiber and seven slicer fibres are separated by one or more blank fibres of the same size. All these fibres have the Acrylate buffer removed for several cm so they can be packed as closely as possible to one another.

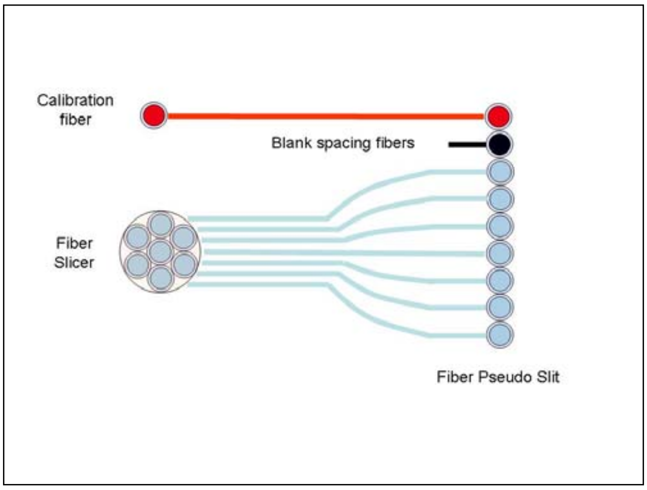


**Figure 16: Fiber slicer pseudo slit with calibration fiber**

The total length of this assembly will be a meter or less. This is critical as we are using very small cladding thickness which can lead to loss due to waveguide leakage. Schotz et al. ( in *Fiber Optics in Astronomy III*, ASP Conference Series, Vol. **152**, p20-31, 1998) compare measurements of the attenuation through infrared of fibres with a 10 and 20 micron thick cladding that show the increased loss in the thinner cladding. Figure 17 below shows an attenuation plot derived from the data they presented with an additional extrapolation for a 5 micron thick cladding that we propose to use. We have assumed the differential loss in going from 10 to 5 microns is the same as going from 20 to 10 microns in this model. This may not be the case and we feel this needs to be tested. We have 5 meter test samples of Polymicro FIP 100110125, FIP100120140 and FIP 100140250 which have 5, 10 and 20 micron thick claddings respectively. We will mount these side by side and test them to retire any risk associated with this approach to a fiber slicer. Increasing the cladding thickness to 20 microns would reduce the packing fraction Efficiency to ~39% which is unacceptably low.

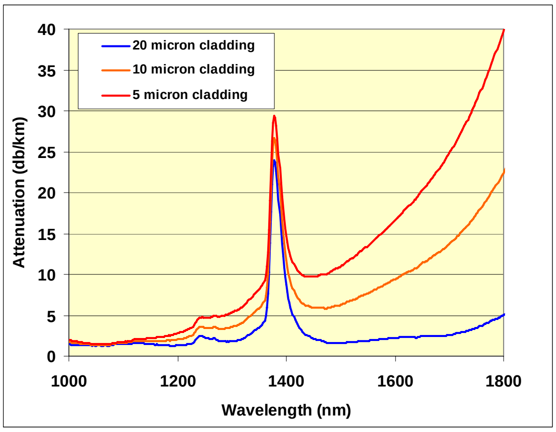


**Figure 17: Attenuation with cladding thickness**

Figure 18 on the right uses the attenuations in Figure 17 to estimate the transmission in the 1 meter fibres that will be used in the scrambler. If our estimates above are correct, the loss for a 5 micron cladding is not at all serious for very small lengths. At this point in time we feel safe in adopting a 100 micron core, 110 micron cladding fiber as our baseline in the fiber slicer. It is important to note that the measured FWHM of a circular fiber is significantly less that the diameter. On our medium resolution spectrograph we measure the FWHM at 78% of whate the projected diameter predicts. Bershady et al (Ap.J Suppl. 156, 311, 2005) measure a similar value of 0.8. Thus we use 80% of the fiber diameter as the effective "slit width".

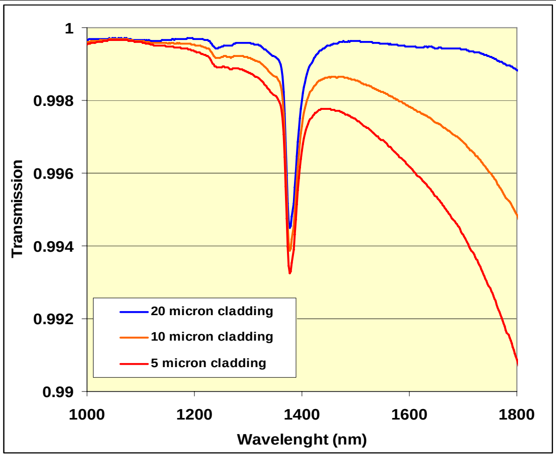


**Figure 18: Transmission with cladding thickness**

We have constructed a prototype of the fiber slicer following these principles. This slicer is currently being used on the PRVS pathfinder instrument at Penn State. This uses 100 micron core, 125 micron cladding diameter fibres and thus has a 49% geometrical throughput. Figure 19 shows the polished input end and Figure 20 shows the pseudo slit which has two calibration fibres, one above and one below the 7 slicer fibres each separated by a blank fiber. Figure 21 shows the slicer/calibration fiber assembly with laser light illuminating the slicer input. The laser output indicated quite decent FRD though we have yet to quantify this precisely. Studies of FRD to date have not shown dependence on wavelength and we would expect similar behaviour in the 0.95-1.75 micron region. Due to the fabrication method utilized for the slicer and pseudo slit, we expect that these will expend most of the FRD budget which is 10%. That is for the f/5.5 input at the Fiber Deployment and Acquisition unit we have a goal for output of the pseudo slit to be f/5.0.

**Figure 19: Fiber Slicer Input**

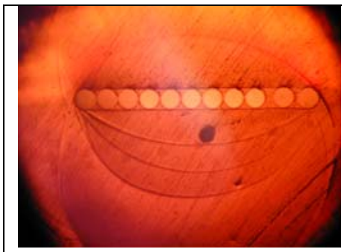

**Figure 20: Fiber Slicer Pseudo Slit**

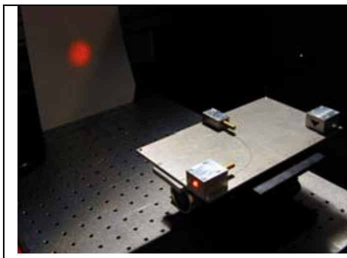

**Figure 21: Slicer Pseudo Slit FRD**

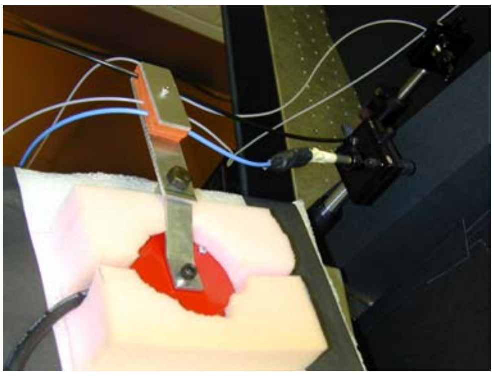

**Figure 22: PRVS Pathfinder Fiber Agitator**

### 3.2.8 Fiber Agitation System

We have yet to complete a comprehensive design of the fiber agitation system. That said, we will use as a guide the system we have in place on the PRVS pathfinder at Penn State. We use a standard commercial mechanical agitator that works at 60 Hz and has variable amplitude. As is illustrated in Figure 22, this is attached to the fibres by way of a padded clamp. We will have to evaluate how this works with the Stainless Steel spiral wrap cables we have outlined.

## 3.3 CONTROL SYSTEM INTERFACES

The only controls system interfaces are the TBD interfaces to the two fiber agitators. At a minimum there will be a on/off control for both and at a maximum an addition amplitude and frequency control for each.

## 3.4 RISKS

There is abundant experience in building fiber feeds for astronomical spectrographs. However, applications in the NIR are much more limited and there is virtually no precedent for high precision spectroscopy such as that proposed in the PRVS. Our concept design is based on straightforward extrapolation from our experience in the visible but some aspects are not yet proven and thus pose risk. We list below what we view as the major risk in this subsystem:

1. Exceeding FRD budget in the science fiber and/or fiber slicer
2. Mechanical Scrambling is inadequate requiring an optical scrambler
3. Controlling modal noise with mechanical scrambler
4. Low number of modes at long wavelength end of bandpass
5. Transmission efficiency of fiber slicer beyond 1 micron is inadequate due to waveguide leakage

We outline in the following paragraphs how we propose to address these risks.

Risk 1 is perhaps the largest in this subsystem. While FRD budgets of 10% are achievable they will be difficult to achieve in this application as there are two segments to the signal fiber; a long large core diameter fiber from the FDAS to the spectrograph and a short bundle of small core diameter fibres in a cooled evacuated environment inside the spectrograph enclosure. While we are confident we can achieve good FRD properties in the 300 micron core fiber, the fiber slicer will be in a vacuum and cooled and we do not have experience in how the epoxy techniques we use will behave in this environment. In the preliminary design phase we will construct and test a prototype under the expected conditions in the spectrograph. If we determine that FRD will not be acceptable, we will move to a Bowen Walraven slicer. Another alternative to a Bowen_Walrave slicer is to use a lenslet array to re-image onto the seven slicer fibres. A hexagonal array with a ~2 mm pitch and ~f/5.3 lenses would allow the individual fibres making up the pseudo slit to be more widely separated and potentially easing FRD in this segment.

Risk 2 will also be addressed early in the preliminary design phase simultaneous with Risk 3. We will conduct tests to measure the scrambling for prototype 300 mircon fiber cable and fiber slicer. If mechanical scrambling is not sufficient, we can revert to an optical double scrambler along the lines of that tested by Hunter and Ramsey (PASP, 104, 1244, 1992).

Risks 3 & 4 are important to retire as early as possible. The risk lies principally in the 100 microns core fiber. Inspection of **Error! Reference source not found.** shows that modal noise limited S/N is still ~300 at the longest wavelength. During the preliminary design phase we will test modal nose remediation out to 1.7 microns in 100 microns core fibres as well as analyse the effects of a Bowen Walraven slicer vignetting on the modal noise from a 300 microns fiber.

Risk 5 is fundamental to the design approach and will be addressed by direct experiment. We already have 5 meter samples of 100 micron core fiber with 5, 10 and 20 micron thick cladding. These will be tested in the PRVS pathfinder to measure the relative transmission in the H Band.